Structural Engineering and Mechanics, *Vol. 72, No. 2 (2019) 229-244*
DOI: https://doi.org/10.12989/sem.2019.72.2.229

Flapwise and non-local bending vibration of the rotating beams

Mehrdad Mohammadnejad*[1] and Hamed Saffari[2]

[1]*Department of Civil Engineering, Birjand University of Technology, Birjand, Iran*
[2]*Department of Civil Engineering, Faculty of Engineering, Shahid Bahonar University of Kerman, Kerman, Iran*

(Received July 15, 2018, Revised May 12, 2019, Accepted May 30, 2019)

Abstract. Weak form integral equations are developed to investigate the flapwise bending vibration of the rotating beams. Rayleigh and Eringen nonlocal elasticity theories are used to investigate the rotatory inertia and Size-dependency effects on the flapwise bending vibration of the rotating cantilever beams, respectively. Through repetitive integrations, the governing partial differential equations are converted into weak form integral equations. The novelty of the presented approach is the approximation of the mode shape function by a power series which converts the equations into solvable one. Substitution of the power series into weak form integral equations results in a system of linear algebraic equations. The natural frequencies are determined by calculation of the non-trivial solution for resulting system of equations. Accuracy of the proposed method is verified through several numerical examples, in which the influence of the geometry properties, rotatory inertia, rotational speed, taper ratio and size-dependency are investigated on the natural frequencies of the rotating beam. Application of the weak form integral equations has made the solution simpler and shorter in the mathematical process. Presented relations can be used to obtain a close-form solution for quick calculation of the first five natural frequencies of the beams with flapwise vibration and non-local effects. The analysis results are compared with those obtained from other available published references.

Keywords: flapwise, size-dependency; weak form integral equation; natural frequency; Rayleigh beam; nonlocal elasticity theory

1. Introduction

The vibration of continuous systems is always encountered in engineering practices. According to the history of structural dynamics, Bernoulli-Euler, Rayleigh and Timoshenko beams theories have been proposed for characterization of elastic beams vibration. These classical continuum mechanics theories provide good results for flapwise bending vibration of the rotating beams. Rotating beam structures are often used in engineering models like helicopter and turbine blades. In order to build such structures, their natural frequencies and mode shapes need to be calculated accurately. These properties of rotating flexible structures differ significantly from those of non-rotating flexible structures. Centrifugal force due to angular velocity of the blades results in the variation of bending stiffness, which can change the natural frequencies and mode shapes of blades vibration. Also, experimental investigations has proved that the classical beam theories are incapable of predicting mechanical behavior of structures in micron scale due to their size-dependency. In order to investigate the size-dependency effects, Eringen nonlocal elasticity theory has been proposed. In this theory, the stress at a reference point is a functional of the strain field at every point of the domain. In recent years, structural elements such as bars, beams, and plates on micro- or nanoscale have often been used as components in micro- or nanoelectromechanical system. Many continuum mechanics approaches are often employed to study the mechanical behavior of micro- or nanoscale structures. The nonlocal elasticity theory is a modified classical elasticity theory which often applied to analyze the vibration behavior of nanostructures (Lee and Chang 2010).

The size-dependency effects of nanobeams have been investigated by nonlocal continuum theory (Eltaher *et al.* 2012, Eltaher *et al.* 2013-a, Nguyen *et al.* 2015). The buckling behaviors of nonlocal functionally graded (FG) Timoshenko and Euler–Bernoulli beams have been studied (Eltaher *et al.* 2014, Emam 2013, Ghannadpour *et al.* 2013, Eltaher *et al.* 2013-b, Thai 2012, Thai and Vo 2012). The dynamic characteristics of damped viscoelastic nonlocal beams have been investigated (Adhikari *et al.* 2013, Murmu *et al.* 2013). The bending, vibration and buckling of nonlocal elastic nanoplates have been studied (Phadikar and Pradhan 2010). By applying the weak form equations, flapwise frequency analysis of the rotating microbeams connected to a hub by incorporating size effect phenomena has been investigated (Dehrouyeh-Semnani 2015). Free vibration of the rotating tapered cantilever beams with rotatory inertia has been studied and the integral equation method has been proposed to determine the natural frequencies (Tang *et al.* 2015). The dynamic stiffness method for free vibration analysis of a rotating tapered Rayleigh beam has been developed. The effects of centrifugal stiffening, an outboard force, an arbitrary hub

*Corresponding author, Assistant Professor
E-mail: mohammadnejad@birjandut.ac.ir
[a] Professer
E-mail: hsaffari@mail.uk.ac.ir

Copyright © 2019 Techno-Press, Ltd.

ISSN: 1225-4568 (Print), 1598-6217 (Online)

radius and the rotatory inertia (Rayleigh beam) have been included in the analysis (Banerjee and Jackson 2013). A comprehensive dynamic model of a rotating hub–functionally graded material (FGM) beam system has been developed based on a rigid–flexible coupled dynamics theory. The dynamic stiffening effect of the rotating hub–FGM beam system has been captured by a second-order coupling term that represents longitudinal shrinking of the beam caused by the transverse displacement (Li *et al.* 2014). The nonlinear von Karman strain and the corresponding linear stress have been used to consider the stiffening effect due to rotation of a rotating cantilever beam (Kim *et al.* 2013). Using the power series solution, the natural frequency of the flapwise bending vibration, and coupled lagwise bending and axial vibration has been investigated for the rotating Euler beams (Huang *et al.* 2010). The governing differential equation of the rotating beam has been reduced to that of a stiff string by assumption of the constant centrifugal force. The solution has been enhanced with a polynomial term and has been used in the Rayleigh's method (Ganesh and Ganguli 2013). The flapwise bending free vibration problem for rotating nano-tubes has been investigated. The small scale effects on the nanotube model have been investigated based on the nonlocal elasticity theory. In this model the effects of transverse shear deformation and rotatory inertia have been accounted (Narendar 2012). The small scale effect on axial vibration of non-uniform and non-homogeneous nanorods has been studied by using the theory of nonlocal elasticity (Chang 2013). Using differential quadrature method, free vibration of nanobeams based on different beam theories like Euler–Bernoulli, Timoshenko, Reddy and Levinson in conjunction with nonlocal elasticity theory have been investigated (Behera and Chakraverty 2015). The natural frequencies of the flapwise bending vibrations of a non-uniform rotating nanocantilever has been calculated, considering the true spatial variation of the axial force due to the rotation (Aranda-Ruiz *et al.* 2012). The flapwise bending–vibration characteristics of a rotating nanocantilever have been investigated. Employing Eringen's nonlocal elasticity theory and differential quadrature method, the nondimensional nonlocal frequencies have been obtained (Pradhan and Murmu 2010). Using three-dimensional nonlocal elasticity theory of Eringen, the closed-form solutions have been presented for in-plane and out-of-plane free vibration of simply supported functionally graded (FG) rectangular micro/nano plates (Salehipour *et al.* 2014). Using nonlocal elasticity theory, the buckling and vibration of nanoplates have been investigated (Aksencer and Aydogdu 2011). Using the nonlocal elastic theory, the natural frequency of a nonuniform nanocantilever beam with consideration of surface effects has been studied (Lee and Chang 2010). Using nonlocal elasticity theory and differential quadrature method, the vibration response of nanocantilever with non-uniformity in the cross sections has been investigated (Murmu and Pradhan 2009). Nonlocal elastic rod model has been developed and has been applied to investigate the small-scale effect on axial vibration of nanorods (Aydogdu 2009). The weak form integral equations have been developed for free vibration analysis of non-prismatic Euler–Bernoulli and Rayleigh beams under variable axial force, non-prismatic shear beam, axial vibration of a non-prismatic bar with and without end discrete spring, torsional vibration of a bar with an attached mass moment of inertia, flexural vibration of the beam with laterally distributed elastic springs and buckling analysis of non-prismatic beams (Mohammadnejad 2015, Saffari *et al.* 2012, Saffari and Mohammadnejad 2015). A closed form solution for both natural frequency and buckling load of nonlocal FG beams resting on nonlinear elastic foundation has been presented (Niknam and Aghdam 2014). A modified nonlocal theory of Eringen has been proposed for analysis of functionally graded (FG) materials at micro/nano scale (Salehipour *et al.* 2015). Bending, buckling, vibrations, and wave propagation of nanobeams modeled according to the nonlocal elasticity theory of Eringen have been investigated (Eltaher, *et al.* 2016). A modified functionally graded beam theory based on the neutral axis has been exploited to investigate natural frequencies of macro/nanobeams (Eltaher, *et al.* 2013). The resonance frequencies of size dependent regular square perforated nonlocal nanobeam has been studied (Eltaher, *et al.* 2018). The free vibration of nonlinear material graduations of a nanobeam based on the nonlocal Timoshenko theory using finite element method has been investigated (Eltaher, *et al.* 2014). Mechanical behaviors of size-dependent nanobeams on the basis of the higher order gradient model has been investigated (Eltaher, *et al.* 2014).

In this paper, the weak form integral equations for flapwise bending vibration analysis of the rotating beams are developed. Rayleigh beam theory is used to investigate flapwise bending vibration of the rotating beams with rotatory inertia effects. After this, Size-dependency effects are investigated using Eringen nonlocal elasticity theory. The governing differential equation for free vibration of a beam with variable stiffness and mass is a partial differential equation with variable coefficients. Many mathematical techniques may be employed to determine the numerical solution or the approximate solution for this equation. The presented approach in this paper for conversion of the governing partial differential equation into solvable one is based on the conversion of the governing equation into its weak form. A differential equation includes a function and its derivatives. The weak form of the differential equation is obtained through the repetitive integration of the initial equation. The integration continues till the resulting integral equation, includes only the function itself after the last integration stage; derivatives of the function will have been eliminated due to the integration. The solution of the weak form of the differential equation instead of the initial equation has many applications in the finite elements analysis.

Free vibration analysis of the rotating beams includes two general fields such as the finite elements approach (or numerical approach) and approximate analytical approach. The finite element approach and numerical approach are based on the discrete model and have to solve thousands of linear simultaneous equations to give quantitative results in detail. So they are a powerful tool for analysis and design at

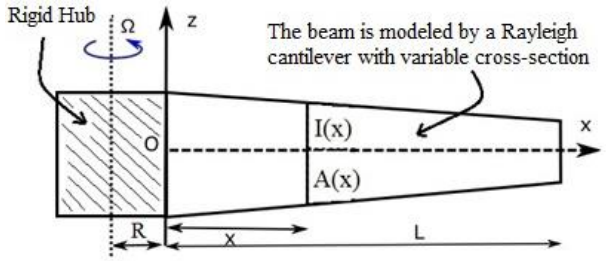

Fig. 1 Flapwise bending vibration of the rotating tapered Rayleigh beam

the detailed and final design stage. Presented method in this paper is an analytical approximate method based continuum approach that gives insight into characteristics of free vibration. It is simple and accurate enough that can be routinely used for the preliminary stage of analysis. The advantages of both analytical and approximate methods of continuum modeling may not be replaced by the discrete modeling of finite element analysis. It should be noticed present method is a combination of exact analytical approach (repetitive integration stages) and approximate approach (approximation of the mode shape function using a power series) based on the continuum approach.

Using four successive integration, the governing differential equation which is based on the fourth order derivative of the mode shape function of the vibration is converted into its weak form integral equation. This method has been used in Ref (Huang and Li 2010) for calculation of the natural frequencies of axially functionally graded Bernoulli-Euler beams with non-uniform cross-section. After four successive integration, the resulting equation is based on the mode shape function. Therefore, the mode shape function is approximated using a power series. Substitution of the power series into weak form integral equations results in a system of linear algebraic equations. The natural frequencies are determined by calculation of the non-trivial solution for resulting system of equations. In Section 5, the results of proposed method are compared with those obtained by Refs (Tang *et al.* 2015, Banerjee and Jackson 2013, Pradhan and Murmu 2010). In Ref (Tang *et al.* 2015), using a mathematical relation, the fourth order governing equation has been converted into a second order one based on the bending moment function. After this, using two successive integration, the second order equation has been converted into an integral equation based on the bending moment function. The bending moment function has been approximated using a power series. In Ref (Banerjee and Jackson 2013), the dynamic stiffness method has been used for calculation of the natural frequencies.

2. Flapwise bending vibration of the rotating tapered Rayleigh beam

2.1 Conversion of the governing equation into its weak form

In Fig. 1, a cantilever tapered beam of length L which is fixed at point o to a rigid hub with radius R, is shown. The beam is modeled by a Rayleigh cantilever with variable cross-section. Rotatory inertia is considered. The beam is assumed to rotate in the counter-clockwise direction at a constant angular velocity Ω.

$$\begin{aligned}&\frac{\partial^2}{\partial x^2}\left[EI(\mathrm{x})\frac{\partial^2 W(\mathrm{x},t)}{\partial x^2}\right]+\rho A(\mathrm{x})\frac{\partial^2 W(\mathrm{x},t)}{\partial t^2}\\&-\frac{\partial}{\partial x}\left[T(\mathrm{x})\frac{\partial W(\mathrm{x},t)}{\partial x}\right]-\frac{\partial}{\partial x}\left[\rho I(\mathrm{x})\frac{\partial^3 W(\mathrm{x},t)}{\partial x\partial t^2}\right]+\\&\Omega^2\frac{\partial}{\partial x}\left[\rho I(\mathrm{x})\frac{\partial W(\mathrm{x},t)}{\partial x}\right]=0\qquad 0\le x\le L\end{aligned}\tag{1}$$

Tang *et al.* (2015) have used Hamilton's variation principle in order to obtain the governing differential equation for flapwise bending vibration of the rotating non-uniform Rayleigh beam as follows (refer to Tang *et al.* 2015 for process of the calculation of the governing equation in more details):

In which $W(\mathrm{x},t)$, $A(\mathrm{x})$, $I(\mathrm{x})$, ρ, L and E are the displacement in the flapwise direction, variable cross-sectional area, second moment of the cross-sectional area, the mass density of the beam, beam length and the modulus of elasticity respectively. T(x) is the centrifugal tension force at a distance x from the center which can be calculated as follows:

$$T(x)=\rho\Omega^2\int_x^L A(x)\left(R+x\right)dx\tag{2}$$

T(x) is due to the rotational motion of the beam. If there was an axial force acting on the cross section of the beam, that force is added to T(x). The assumptions for the tapered beam are as follows

$$\begin{cases}I(x)=I_0(1-c\dfrac{x}{L})^{n+2}=I_0\ f_1(x)\\A(x)=A_0(1-c\dfrac{x}{L})^{n}=A_0\ f_2(x)\end{cases}\tag{3}$$

Where A_0 and I_0 are the cross-sectional area and second moment of the cross-sectional area at x=0. c is a constant called the taper ratio which must be such that $c < 1$. Values of n=1 or 2 cover the most practical cases because n=1 gives linear variation of the area of the cross-section and cubic variation of the second moment of area along the length, whereas n= 2 are the second and fourth orders. If motion is represented by a harmonic vibration, the flapwise displacement is obtained using the following relation

$$W\left(x,t\right)=\phi(x)e^{\mathrm{i}\omega t}\tag{4}$$

Where ϕ(x) and ω are the mode shape function and the natural frequency of the beam, respectively. $i^2=-1$ is applied. For further convenience, the following dimensionless variables are introduced:

$$\begin{cases}\xi=\dfrac{x}{L}\ ,\ \phi\left(\xi\right)=\dfrac{\phi\left(x\right)}{L}\ ,\ \mathrm{r}_0=\dfrac{R}{L}\ ,\ \lambda^2=\dfrac{\rho A_0\omega^2L^4}{EI_0}\\\eta^2=\dfrac{\rho A_0\Omega^2L^4}{EI_0}\ ,\ r^2=\dfrac{I_0}{A_0L^2}\end{cases}\tag{5}$$

Where ξ, $\phi(\xi)$ and r_0 are the dimensionless parameters for the local location, mode shape function and the hub radius respectively. r, η and λ are the dimensionless parameters related to the inverse of slenderness ratio, the angular velocity and the natural frequency respectively. Substitution of relations (2-5) into Eq. (1) leads to a single-variable equation in terms of location, as follows

$$\frac{d^2}{d\xi^2}\left[f_1(\xi)\frac{d^2\phi(\xi)}{d\xi^2}\right]-\lambda^2 f_2(\xi)\phi(\xi)+ \lambda^2 r^2\frac{d}{d\xi}\left[f_1(\xi)\frac{d\phi(\xi)}{d\xi}\right]-\eta^2\frac{d}{d\xi}\left[t(\xi)\frac{d\phi(\xi)}{d\xi}\right]+ \eta^2 r^2\frac{d}{d\xi}\left[f_1(\xi)\frac{d\phi(\xi)}{d\xi}\right]=0 \qquad 0\le\xi\le 1 \tag{6}$$

In which the function

$$t\left(\xi\right)=\int_{\xi}^{1} f_2(s)(r_0+s)ds$$

is applied. Eq. (6) is, in fact, the free vibration equation for flapwise bending vibration of a rotating tapered Rayleigh beam based on the non-dimensional variable ξ. In order to transform Eq. (6) to its weak form, both sides of Eq. (6) are integrated twice with respect to ξ within the range 0 to ξ. The results are the integral equations as follows

$$\frac{d}{d\xi}\left[f_1(\xi)\frac{d^2\phi(\xi)}{d\xi^2}\right]-\lambda^2\int_0^{\xi} f_2(s)\phi(s)\,\mathrm{ds}+ \lambda^2 r^2 f_1(\xi)\frac{d\phi(\xi)}{d\xi}-\eta^2 t(\xi)\frac{d\phi(\xi)}{d\xi}+ \eta^2 r^2 f_1(\xi)\frac{d\phi(\xi)}{d\xi}=C_1 \tag{7}$$

$$f_1(\xi)\frac{d^2\phi(\xi)}{d\xi^2}-\lambda^2\int_0^{\xi}(\xi-s)\, f_2(s)\phi(s)\,\mathrm{ds}+ \lambda^2 r^2 f_1(\xi)\phi(\xi)-\lambda^2 r^2\int_0^{\xi} f_1'(s)\phi(s)\,\mathrm{ds}-\eta^2 t(\xi)\phi(\xi) +\eta^2\int_0^{\xi} t'(s)\phi(s)\,\mathrm{ds}+\eta^2 r^2 f_1(\xi)\phi(\xi)- \eta^2 r^2\int_0^{\xi} f_1'(s)\phi(s)\,\mathrm{ds}=C_1\xi+C_2 \tag{8}$$

Further, integration from both sides of Eq. (8) twice with respect to ξ from 0 to ξ yields

$$f_1(\xi)\frac{d\phi(\xi)}{d\xi}-f_1'(\xi)\phi(\xi)+\int_0^{\xi} f_1''(s)\phi(s)ds- \frac{\lambda^2}{2}\int_0^{\xi}(\xi-s)^2\, f_2(s)\phi(s)\,\mathrm{ds}+\lambda^2 r^2\int_0^{\xi} f_1(s)\phi(s)\,\mathrm{ds} -\lambda^2 r^2\int_0^{\xi}(\xi-s)\, f_1'(s)\phi(s)\,\mathrm{ds}-\eta^2\int_0^{\xi} t(s)\phi(s)\,\mathrm{ds}+ \eta^2\int_0^{\xi}(\xi-s)t'(s)\phi(s)\,\mathrm{ds}+\eta^2 r^2\int_0^{\xi} f_1(s)\phi(s)ds -\eta^2 r^2\int_0^{\xi}(\xi-s)\, f_1'(s)\phi(s)\,\mathrm{ds}=\frac{C_1}{2}\xi^2+C_2\xi+C_3 \tag{9}$$

$$f_1(\xi)\phi(\xi)-2\int_0^{\xi} f_1'(s)\phi(s)ds+ \int_0^{\xi}(\xi-s)\, f_1''(s)\phi(s)ds-\frac{\lambda^2}{6}\int_0^{\xi}(\xi-s)^3\, f_2(s)\phi(s)\,\mathrm{ds}+ \lambda^2 r^2\int_0^{\xi}(\xi-s)\, f_1(s)\phi(s)\,\mathrm{ds}- \frac{\lambda^2 r^2}{2}\int_0^{\xi}(\xi-s)^2\, f_1'(s)\phi(s)\,\mathrm{ds}- \eta^2\int_0^{\xi}(\xi-s)t(s)\phi(s)\,\mathrm{ds} +\frac{\eta^2}{2}\int_0^{\xi}(\xi-s)^2 t'(s)\phi(s)\,\mathrm{ds}+ \eta^2 r^2\int_0^{\xi}(\xi-s)\, f_1(s)\phi(s)ds- \frac{\eta^2 r^2}{2}\int_0^{\xi}(\xi-s)^2\, f_1'(s)\phi(s)\,\mathrm{ds} =\frac{C_1}{6}\xi^3+\frac{C_2}{2}\xi^2+C_3\xi+C_4 \tag{10}$$

Eq. (10) is the integral equation of the weak form of Eq. (6). As can be seen, Eq. (6) includes a fourth order derivative of the mode shape function and after four successive integrations, Eq. (10) includes only the mode shape function itself. In Eq. (10) C_1, C_2, C_3 and C_4 are the integration constants which are determined through boundary conditions of both ends of the beam. Eqs. (7-10) are applicable for determination of the integration constants.

2.2 Boundary conditions

The following boundary conditions must be considered for the cantilevered beam:

$$\begin{cases} x=0 & W(0,\mathrm{t})=0 \\ & or \\ \xi=0 & \phi(0)e^{i\omega t}=0 \;\rightarrow\; \phi(0)=0 \\ x=0 & \dfrac{\partial W}{\partial x}(0,\mathrm{t})=0 \\ & or \\ \xi=0 & \dfrac{\mathrm{d}\phi}{L\mathrm{d}\xi}(0)e^{i\omega t}=0 \;\rightarrow\; \dfrac{\mathrm{d}\phi}{\mathrm{d}\xi}(0)=0 \end{cases} \tag{11, 12}$$

Also, the following boundary conditions are established for flapwise bending vibration of the tapered cantilevered Rayleigh beam

$$\begin{cases} x=L & EI(\mathrm{x})\dfrac{\partial^2 W(\mathrm{x},t)}{\partial x^2}=0 \\ & \downarrow \\ \xi=1 & \dfrac{\mathrm{d}^2\phi(\xi)}{\mathrm{d}\xi^2}=0 \end{cases} \tag{13}$$

$$\begin{cases} x=L & \dfrac{\partial}{\partial x}\left[EI(\mathrm{x})\dfrac{\partial^2 W(\mathrm{x},t)}{\partial x^2}\right]-\rho I(\mathrm{x})\dfrac{\partial^3 W(\mathrm{x},t)}{\partial x\partial t^2}+ \\ & \Omega^2\rho I(\mathrm{x})\dfrac{\partial W(\mathrm{x},t)}{\partial x}=0 \\ & \downarrow \\ \xi=1 & \dfrac{d}{d\xi}\left[f_1(\xi)\dfrac{d^2\phi(\xi)}{d\xi^2}\right]+\lambda^2 r^2 f_1(\xi)\dfrac{d\phi(\xi)}{d\xi}+ \\ & \eta^2 r^2 f_1(\xi)\dfrac{d\phi(\xi)}{d\xi}=0 \end{cases} \tag{14}$$

Application of the condition (11) at Eq. (10) and conditions (11) and (12) at Eq. (9) leads to

$$C_3=C_4=0 \tag{15}$$

Also, Application of the condition (13) at Eq. (8) leads to

$$\begin{aligned} &-\lambda^2\int_0^1(1-s)\,f_2(\mathrm{s})\phi(s)ds+\lambda^2 r^2 f_1(1)\phi(1)- \\ &\lambda^2 r^2\int_0^1 f_1'(s)\phi(s)ds \\ &+\eta^2\int_0^1 t'(s)\phi(s)ds+\eta^2 r^2 f_1(1)\phi(1)- \\ &\eta^2 r^2\int_0^1 f_1'(s)\phi(\mathrm{s})=C_1+C_2 \end{aligned} \tag{16}$$

Regarding $t(1)=0$, substitution of the condition (14) into Eq. (7) yields:

$$-\lambda^2\int_0^1 f_2(\mathrm{s})\phi(s)ds=C_1 \tag{17}$$

It is easily found that in Eq. (16), $\phi(1)$ is also unknown. As a consequence, another independent equation is needed for uniquely determining C_2. Substitution of C_1, C_3 and C_4 into Eq. (10) results in an equation which can be used for calculation of $\phi(\xi)$ as follows:

$$f_1(\xi)\phi(\xi)+\int_0^\xi k_1(\xi,s)\phi(s)\,\mathrm{ds}=\frac{C_1}{6}\xi^3+\frac{C_2}{2}\xi^2 \tag{18}$$

In which

$$\begin{aligned} &k_1(\xi,s)=-2\int_0^\xi f_1'(s)\phi(s)ds+ \\ &\int_0^\xi(\xi-s)\,f_1''(\mathrm{s})\phi(s)ds-\frac{\lambda^2}{6}\int_0^\xi(\xi-s)^3\,f_2(s)\phi(\mathrm{s})\,\mathrm{ds}+ \\ &\lambda^2 r^2\int_0^\xi(\xi-s)\,f_1(s)\phi(\mathrm{s})\,\mathrm{ds}- \\ &\frac{\lambda^2 r^2}{2}\int_0^\xi(\xi-s)^2\,f_1'(s)\phi(\mathrm{s})\,\mathrm{ds}- \\ &\eta^2\int_0^\xi(\xi-s)t(s)\phi(\mathrm{s})\,\mathrm{ds}+ \\ &\frac{\eta^2}{2}\int_0^\xi(\xi-s)^2\,t'(s)\phi(\mathrm{s})\,\mathrm{ds}+ \\ &\eta^2 r^2\int_0^\xi(\xi-s)\,f_1(s)\phi(s)ds- \\ &\frac{\eta^2 r^2}{2}\int_0^\xi(\xi-s)^2\,f_1'(s)\phi(\mathrm{s})\,\mathrm{ds} \end{aligned} \tag{19}$$

$\phi(1)$ can be calculated by setting $\xi=1$ into Eq. (18). The result is as follows

$$\phi(1)=-\frac{1}{f_1(1)}\int_0^1 k_1(1,s)\phi(\mathrm{s})\,\mathrm{ds}+\frac{C_1}{6f_1(1)}+\frac{C_2}{2f_1(1)} \tag{20}$$

By substitution of C_1 and $\phi(1)$ (Eqs. 17 and 20) into Eq. (16), the integration constant C_2 is calculated as follows

$$C_2=\alpha\int_0^1 g(s)\phi(s)ds \tag{21}$$

Where

$$\begin{cases} g(s)=\dfrac{-\lambda^2\alpha_1}{6f_1(1)}f_2(\mathrm{s})-\dfrac{\alpha_1}{f_1(1)}k_1(1,s)-\lambda^2(1-s)f_2(\mathrm{s})- \\ \lambda^2 r^2 f_1'(\mathrm{s})+\eta^2 t'(\mathrm{s})-\eta^2 r^2 f_1'(\mathrm{s})+\lambda^2 f_2(\mathrm{s}) \\ \alpha=\dfrac{2f_1(1)}{2f_1(1)-\alpha_1} \\ \alpha_1=\lambda^2 r^2 f_1(1)+\eta^2 r^2 f_1(1) \end{cases} \tag{22}$$

Substitution of the integration constants C_1, C_2, C_3 and C_4 into Eq. (10) results in an integral equation in $\phi(\xi)$ as follows:

$$f_1(\xi)\phi(\xi)+\int_0^\xi k_1(\xi,s)\phi(\mathrm{s})\,\mathrm{ds}+\int_0^1 k_2(\xi,s)\phi(\mathrm{s})\,\mathrm{ds}=0 \tag{23}$$

In which

$$k_2(\xi,s)=\frac{\lambda^2}{6}\xi^3 f_2(\mathrm{s})-\frac{\alpha}{2}\xi^2 g(s) \tag{24}$$

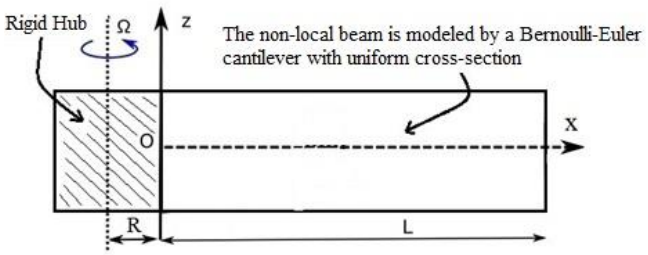

Fig. 2 Flapwise bending vibration of the non-local rotating beam

Eq. (23) is the weak form integral equation for flapwise bending vibration of the rotating cantilevered tapered Rayleigh beam. The mode shape function $\phi(\xi)$ is the only unknown parameter in the integral equation (23).

3. Flapwise bending vibration of the non-local rotating Bernoulli-Euler beam

3.1 Conversion of the governing equation into its weak form

The classical beam theories cannot predict mechanical behavior of structures in micron scale due to their size-dependency. In order to investigate size-dependency effects on the flapwise bending vibration of the rotating beam, Eringen nonlocal elasticity theory is used. In this theory, the stress at a reference point is a functional of the strain field at every point of the domain. The size-dependency effects are taken into account using the term $(e_0 a)$ which is called the nonlocal parameter or the scale-coefficient. In this section, the flapwise bending vibration of a rotating non-local Bernoulli-Euler beam is investigated. The size-dependency effects are considered using the nonlocal elasticity theory. It is assumed that the beam has a uniform section along the length (Fig. 2).

The governing differential equation for free vibration of such beam is given as follows (Pradhan and Murmu 2010):

$$EI\frac{\partial^4 W(\mathrm{x},t)}{\partial x^4}+\rho A\frac{\partial^2 W(\mathrm{x},t)}{\partial t^2}-\frac{\partial}{\partial x}\left[T(\mathrm{x})\frac{\partial W(\mathrm{x},t)}{\partial x}\right]+\left(e_0 a\right)^2\frac{\partial^2}{\partial x^2}\left[\frac{\partial}{\partial x}\left(T(\mathrm{x})\frac{\partial W(\mathrm{x},t)}{\partial x}\right)-\rho A\frac{\partial^2 W(\mathrm{x},t)}{\partial t^2}\right]=0 \qquad 0\le x\le L \tag{25}$$

If motion is represented by a harmonic vibration, the transverse displacement is obtained using the following relation:

$$W\left(x,t\right)=\phi(x)e^{\mathrm{i}\omega t} \tag{26}$$

Where $\phi(x)$ and ω are the mode shape function and the natural frequency of the beam respectively. Regarding the non-dimensional parameters introduced in relations (5), substitution of Eq. (26) into Eq. (25) results in a single-variable equation in terms of location as follows:

$$\frac{d^4\phi(\xi)}{d\xi^4}-\eta^2\frac{d}{d\xi}\left[t(\xi)\frac{d\phi(\xi)}{d\xi}\right]-\lambda^2\phi(\xi)+\psi^2\lambda^2\frac{d^2\phi(\xi)}{d\xi^2}+\psi^2\eta^2\frac{d^3}{d\xi^3}\left[t(\xi)\frac{d\phi(\xi)}{d\xi}\right]=0 \qquad 0\le\xi\le 1 \tag{27}$$

In which $\psi^2=\left(\frac{e_0 a}{L}\right)^2$ is the non-dimensional parameter for nonlocal parameter and the function $t\left(\xi\right)=\int_{\xi}^{1}(r_0+s)ds$ is applied. Eq. (27) is, in fact, the free vibration equation of the flapwise bending vibration of the non-local rotating Bernoulli-Euler beam based on the non-dimensional variable ξ. In order to transform Eq. (27) to its weak form, both sides of Eq. (27) are integrated twice with respect to ξ within the range 0 to ξ. The results are the integral equations as follows:

$$\frac{d^3\phi(\xi)}{d\xi^3}-\eta^2 t(\xi)\frac{d\phi(\xi)}{d\xi}-\lambda^2\int_0^{\xi}\phi(s)ds+\psi^2\lambda^2\frac{d\phi(\xi)}{d\xi}-\psi^2\eta^2\frac{d\phi(\xi)}{d\xi}+2\psi^2\eta^2 t'(\xi)\frac{d^2\phi(\xi)}{d\xi^2}+\psi^2\eta^2 t(\xi)\frac{d^3\phi(\xi)}{d\xi^3}=C_1 \tag{28}$$

$$\frac{d^2\phi(\xi)}{d\xi^2}-\eta^2 t(\xi)\phi(\xi)+\eta^2\int_0^{\xi}t'(\mathrm{s})\phi(\mathrm{s})ds-\lambda^2\int_0^{\xi}(\xi-s)\phi(s)ds+\psi^2\lambda^2\phi(\xi)+\psi^2\eta^2 t'(\xi)\frac{d\phi(\xi)}{d\xi}+\psi^2\eta^2 t(\xi)\frac{d^2\phi(\xi)}{d\xi^2}=C_1\xi+C_2 \tag{29}$$

Further, integration from both sides of Eq. (29) twice with respect to ξ from 0 to ξ yields

$$\frac{d\phi(\xi)}{d\xi}-\eta^2\int_0^{\xi}t(s)\phi(s)ds+\eta^2\int_0^{\xi}(\xi-s)t'(\mathrm{s})\phi(\mathrm{s})ds-\frac{\lambda^2}{2}\int_0^{\xi}(\xi-s)^2\phi(s)ds+\psi^2\lambda^2\int_0^{\xi}\phi(s)ds+\psi^2\eta^2 t(\xi)\frac{d\phi(\xi)}{d\xi}=\frac{C_1}{2}\xi^2+C_2\xi+C_3 \tag{30}$$

$$\begin{aligned}&\phi(\xi)-\eta^2\int_0^{\xi}(\xi-s)t(s)\phi(s)ds+\\&\frac{\eta^2}{2}\int_0^{\xi}(\xi-s)^2t'(s)\phi(s)ds-\frac{\lambda^2}{6}\int_0^{\xi}(\xi-s)^3\phi(s)ds+\\&\psi^2\lambda^2\int_0^{\xi}(\xi-s)\phi(s)ds+\psi^2\eta^2t(\xi)\phi(\xi)-\\&\psi^2\eta^2\int_0^{\xi}t'(s)\phi(s)ds=\frac{C_1}{6}\xi^3+\frac{C_2}{2}\xi^2+C_3\xi+C_4\end{aligned}\tag{31}$$

It should be noted that in the equations above $t''(\xi)=-1$ and $t'''(\xi)=0$ have been applied. Eq. (31) is the integral equation of the weak form of Eq. (27). In Eq. (31) C_1, C_2 , C_3 and C_4 are the integration constants which are determined through boundary conditions of both ends of the beam. Eqs. (28-31) are applicable for determination of the integration constants.

3.2 Boundary conditions

The following boundary conditions must be considered for the cantilevered Bernoulli-Euler beam

$$\begin{cases}x=0 \quad W(0,t)=0\\ \qquad\quad or\\ \xi=0 \quad \phi(0)e^{i\omega t}=0 \;\rightarrow\; \phi(0)=0\end{cases}\tag{32}$$

$$\begin{cases}x=0 \quad \dfrac{\partial W}{\partial x}(0,t)=0\\ \qquad\quad or\\ \xi=0 \quad \dfrac{d\phi}{Ld\xi}(0)e^{i\omega t}=0 \;\rightarrow\; \dfrac{d\phi}{d\xi}(0)=0\end{cases}\tag{33}$$

$$\begin{cases}x=L \quad EI\dfrac{\partial^2W(x,t)}{\partial x^2}=0\\ \qquad\quad or\\ \xi=1 \quad \dfrac{d^2\phi(\xi)}{d\xi^2}=0\end{cases}\tag{34}$$

$$\begin{cases}x=L \quad EI\dfrac{\partial^3W(x,t)}{\partial x^3}=0\\ \qquad\quad or\\ \xi=1 \quad \dfrac{d^3\phi(\xi)}{d\xi^3}=0\end{cases}\tag{35}$$

Application of the condition (32) at Eq. (31) and condition (33) at Eq. (30) leads to

$$C_3=C_4=0\tag{36}$$

Regarding $t(1)=0$, Application of the condition (34) at Eq. (29) leads to

$$\begin{aligned}&\psi^2\lambda^2\phi(1)+\psi^2\eta^2t'(1)\frac{d\phi}{d\xi}(1)+\\&\int_0^1\left[\eta^2t'(s)-\lambda^2(1-s)\right]\phi(s)=C_1+C_2\end{aligned}\tag{37}$$

Substitution of the conditions (34) and (35) into Eq. (28) yields

$$\left[\psi^2\lambda^2-\psi^2\eta^2\right]\frac{d\phi}{d\xi}(1)-\lambda^2\int_0^1\phi(s)ds=C_1\tag{38}$$

In Eqs. (37) and (38) $\phi(1)$ and $\dfrac{d\phi}{d\xi}(1)$ are also unknown. As a consequence, two other independent equations are needed for uniquely determining C_1 and C_2. Substitution of C_3 and C_4 into Eq. (31) results in an equation which can be used for calculation of $\phi(\xi)$ as follows

$$\left[1+\psi^2\eta^2t(\xi)\right]\phi(\xi)+\int_0^{\xi}k_1(\xi,s)\phi(s)\,ds=\frac{C_1}{6}\xi^3+\frac{C_2}{2}\xi^2\tag{39}$$

In which

$$\begin{aligned}&k_1(\xi,s)=-\eta^2\int_0^{\xi}(\xi-s)t(s)\phi(s)ds+\\&\frac{\eta^2}{2}\int_0^{\xi}(\xi-s)^2t'(s)\phi(s)ds-\frac{\lambda^2}{6}\int_0^{\xi}(\xi-s)^3\phi(s)ds+\\&\psi^2\lambda^2\int_0^{\xi}(\xi-s)\phi(s)ds-\psi^2\eta^2\int_0^{\xi}t'(s)\phi(s)ds\end{aligned}\tag{40}$$

$\phi(1)$ can be calculated by setting $\xi=1$ into Eq. (39). The result is as follows ($t(1)=0$)

$$\phi(1)=\frac{C_1}{6}+\frac{C_2}{2}-\int_0^1k_1(1,s)\phi(s)\,ds\tag{41}$$

Also, substitution of $C_3=0$ at Eq. (30) and setting $\xi=1$, the following equation is obtained for calculation of $\dfrac{d}{d\xi}\phi(1)$

$$\frac{d\phi}{d\xi}(1)=\frac{C_1}{2}+C_2-\int_0^1g(s)\phi(s)\,ds\tag{42}$$

Where

$$g(s)=\eta^2(\xi-s)t'(s)-\eta^2t(s)-\frac{\lambda^2}{2}(\xi-s)^2+\psi^2\lambda^2\tag{43}$$

By substitution of $\phi(1)$ and $\dfrac{d\phi}{d\xi}(1)$ into Eqs. (37) and (38),

the integration constant C_1 and C_2 are calculated as follows

$$\begin{cases} C_1 = \int_0^1 \left[\dfrac{\alpha_1 p(s) + \alpha_3 q(s)}{\alpha_1\alpha_2 + \alpha_3\alpha_4} \right] \phi(s) ds \\ C_2 = \int_0^1 \left[\dfrac{\alpha_1\alpha_4 p(s) + \alpha_3\alpha_4 q(s)}{\alpha_1^2\alpha_2 + \alpha_1\alpha_3\alpha_4} - \dfrac{q(s)}{\alpha_1} \right] \phi(s) ds \end{cases} \quad (44)$$

In which

$$\begin{cases} p(s) = \eta^2 t'(s) - \lambda^2(1-s) - \psi^2\lambda^2 k_1(1,s) - \\ \psi^2\eta^2 t'(1) g(s) \\ q(s) = -\alpha_1 g(s) - \lambda^2 \\ \alpha_1 = \psi^2\lambda^2 - \psi^2\eta^2 \\ \alpha_2 = 1 - \dfrac{\psi^2\lambda^2}{6} - \dfrac{\psi^2\eta^2 t'(1)}{2} \\ \alpha_3 = 1 - \dfrac{\psi^2\lambda^2}{2} - \psi^2\eta^2 t'(1) \\ \alpha_4 = 1 - \dfrac{\psi^2\lambda^2}{2} + \dfrac{\psi^2\eta^2}{2} \end{cases} \quad (45)$$

Substitution of the integration constants C_1, C_2, C_3 and C_4 into Eq. (31) results in an integral equation in $\phi(\xi)$ as follows

$$\left[1 + \psi^2\eta^2 t(\xi)\right]\phi(\xi) + \int_0^{\xi} k_1(\xi, s)\phi(s)\,ds + \int_0^1 k_2(\xi, s)\phi(s)\,ds = 0 \quad (46)$$

In which

$$k_2(\xi, s) = \left[\frac{-\alpha_1 p(s) - \alpha_3 q(s)}{6\alpha_1\alpha_2 + 6\alpha_3\alpha_4} \right] \xi^3 - \left[\frac{g(s)}{2} + \frac{\lambda^2}{2\alpha_1} + \frac{\alpha_4\alpha_1 p(s) + \alpha_4\alpha_3 q(s)}{2\alpha_1^2\alpha_2 + 2\alpha_1\alpha_3\alpha_4} \right] \xi^2 \quad (47)$$

Eq. (46) is the weak form integral equation for flapwise bending vibration of the rotating non-local Bernoulli-Euler beam. The mode shape function $\phi(\xi)$ is the only unknown parameter in the integral equation (46).

4. Solution of the resulting integral equations

In the preceding sections, the governing differential equations for free flapwise bending vibration of the rotating tapered Rayleigh beam and the rotating non-local Bernoulli-Euler beam have been converted into the integral equation with general form as

$$H(\xi)\phi(\xi) + \int_0^{\xi} k_1(\xi, s)\phi(s)\,ds + \int_0^1 k_2(\xi, s)\phi(s)\,ds = 0 \quad (48)$$

The function $H(\xi)$ has been calculated as $(1-c\xi)^{n+2}$ and $1+\psi^2\eta^2 t(\xi)$ for the rotating tapered Rayleigh beam and the rotating non-local Bernoulli-Euler beam, respectively. The functions $k_1(\xi, s)$ and $k_2(\xi, s)$ have been introduced in the previous sections. The mode shape function $\phi(\xi)$ is the only unknown parameter in the integral equation (48). In order to solve the integral equation (48) and to determine the natural frequencies, the mode shape function is approximated by the following power series

$$\phi(\xi) = \sum_{r=0}^{R} c_r \xi^r \quad (49)$$

Where C_r are unknown coefficients to be determined and R is a given positive integer, which is adopted such that the accuracy of the results are sustained. Introducing Eq. (49) into integral equation (48) leads to

$$\sum_{r=0}^{R} \left[H(\xi)\xi^r + \int_0^{\xi} k_1(\xi, s)s^r\,ds + \int_0^1 k_2(\xi, s)s^r\,ds \right] c_r = 0 \quad (50)$$

Both sides of Eq. (50) are multiplied by ξ^m and integrated subsequently with respect to ξ between 0 and 1. This results in a system of linear algebraic equations in C_r

$$\sum_{r=0}^{R} \left[G(m,r) + K_1(m,r) + K_2(m,r) \right] c_r = 0 \qquad m = 0, 1, 2, ..., R \quad (51)$$

In which functions $G(m,r)$ and $K_i(m,r)$, $(i = 1,2)$ are expressed as follows

$$\begin{cases} G(m,r) = \int_0^1 \xi^{r+m} H(\xi)\,d\xi \\ K_1(m,r) = \int_0^1 \int_0^{\xi} k_1(\xi, s)s^r\xi^m\,ds\,d\xi \\ K_2(m,r) = \int_0^1 \int_0^1 k_2(\xi, s)s^r\xi^m\,ds\,d\xi \end{cases} \quad (52)$$

The system of linear algebraic equations (51) may be expressed in matrix notations as follows:

$$[A]_{(R+1)\times(R+1)} [C]_{(R+1)\times 1} = [0]_{(R+1)\times 1} \quad (53)$$

In which $[A]$ and $[C]$ are the coefficients matrix and unknowns vector respectively. The only unknown parameter in the coefficients matrix $[A]$ is the dimensionless parameter related to the natural frequency of the beam λ. $[C] = 0$ is a trivial solution for the resulting system of equations introduced in (53). The natural frequencies are determined through calculation of a non-trivial solution for

Table 1 the first four dimensionless frequencies of the non-rotating beam with uniform cross section

No. of modes	Euler-Bernoulli beam (r=0)		Rayleigh beam r =1/20		r =1/10	
	present	(Tang *et al.* 2015)	present	(Tang *et al.* 2015)	present	(Tang *et al.* 2015)
First	3.51602	3.51602	3.49575	3.49575	3.43681	3.43681
Second	22.0345	22.03449	21.1907	21.19069	19.1364	19.13637
Third	61.6973	61.69721	56.4863	56.48626	46.4936	46.49355
Fourth	120.904	120.90206	103.825	103.82380	78.2148	78.21309

Table 2 the first three dimensionless frequencies of the beam with n = 1, c = 0.5, r = 0 (Euler-Bernoulli beam), $r = \frac{1}{30}$ (Rayleigh beam)

	η = 1		η = 2	
	Euler-Bernoulli	Rayleigh	Euler-Bernoulli	Rayleigh
	r_0 =0		r_0 =0	
	present	present	present	present
λ_1	3.98662	3.98024	4.4368	4.42885
λ_2	18.474	18.3239	18.9366	18.7813
λ_3	47.4174	46.4755	47.8717	46.9191
	r_0 =2		r_0 =2	
	present	present	present	present
λ_1	4.38668	4.37977	5.74259	5.73313
λ_2	18.8796	18.7259	20.473	20.30461
λ_3	47.8308	46.8804	49.4867	48.5007
	η = 3		η = 4	
	Euler-Bernoulli	Rayleigh	Euler-Bernoulli	Rayleigh
	r_0 =0		r_0 =0	
	present	present	present	present
λ_1	5.09267	5.0826	5.87876	5.86636
λ_2	19.6839	19.5203	20.6852	20.5105
λ_3	48.6191	47.6488	49.6457	48.6512
	r_0 =2		r_0 =2	
	present	present	present	present
λ_1	7.45274	7.44031	9.31032	9.29482
λ_2	22.8795	22.6889	25.8663	25.6482
λ_3	52.1206	51.0776	55.5817	54.4634

resulting system of equations. To achieve this, the determinant of the coefficients matrix of the system has to be vanished. Accordingly, a frequency equation in λ (which is a polynomial function of the order $2(R+1)$) is introduced. The roots of the frequency equation are the dimensionless parameter related to the natural frequency of the beam λ . Given the fact that the mode shape function is approximated by the power series of (49), the results accuracy is improved if more number of the series sentences is taken into account (Larger R is adopted).

5. Numerical examples

In this section, some illustrative examples are given to verify the accuracy and efficiency of the proposed analytical approach. In the numerical examples, the influence of geometry properties, rotatory inertia, rotational speed, taper ratio and size-dependency are investigated on the natural frequencies of the rotating beam. The computer package MATLAB is used to write the codes, based on presented analytical approach.

Table 3-a The first dimensionless frequency of the beam with $n = 1$, $r_0 = 0$

		λ_1			
		$c = 0$	$c = 0.25$	$c = 0.5$	$c = 0.75$
η	1/r	present	present	present	present
0	10	3.4368	3.5722	3.7727	4.13479
	30	3.5070	3.6289	3.8180	4.17189
	50	3.51275	3.6336	3.8217	4.1749
	100	3.5152	3.6356	3.8233	4.1762
	EB	3.516	3.6362	3.8238	4.1766
5	10	6.23179	6.3958	6.6118	6.9577
	30	6.4251	6.5469	6.7286	7.0506
	50	6.4407	6.5591	6.7381	7.0581
	100	6.4473	6.5643	6.7421	7.0613
	EB	6.4495	6.566	6.7434	7.0623
10	10	10.8187	11.0217	11.2631	11.6095
	30	11.1598	11.2889	11.4748	11.7887
	50	11.187	11.3104	11.4919	11.8032
	100	11.1985	11.3195	11.4991	11.8093
	EB	11.2023	11.3225	11.5015	11.8113

Table 3-b The second dimensionless frequency of the beam with $n = 1$, $r_0 = 0$

		λ_2			
		$c = 0$	$c = 0.25$	$c = 0.5$	$c = 0.75$
η	1/r	present	present	present	present
0	10	19.1364	18.2726	17.0975	15.544
	30	21.6477	20.0022	18.1689	16.1093
	50	21.8929	20.1622	18.2634	16.1573
	100	21.9989	20.2309	18.3038	16.1776
	EB	22.0345	20.2539	18.3173	16.1844
5	10	21.8856	21.2756	20.3563	19.0587
	30	24.9737	23.4339	21.7176	19.7979
	50	25.2734	23.6325	21.8372	19.8604
	100	25.4026	23.7176	21.8882	19.887
	EB	25.4461	23.7462	21.9053	19.8959
10	10	28.4787	28.3901	27.916	26.9155
	30	32.9654	31.5417	29.9097	28.0187
	50	33.394	31.828	30.0838	28.1119
	100	33.5784	31.9506	30.1579	28.1514
	EB	33.6404	31.9917	30.1827	28.1646

5.1 Non-rotating Bernoulli-Euler and Rayleigh beams

In this example, the first four dimensionless frequencies of the non-rotating Bernoulli-Euler and Rayleigh beams are calculated. By setting $n = 0$, $\eta = 0$, $r_0 = 0$, $c = 0.5$ and adopting $r = 0$ for Euler–Bernoulli beam and $r = \frac{1}{20}$ or $r = \frac{1}{10}$ for a Rayleigh beam, respectively, the first four dimensionless frequencies of the beam are calculated. The results are presented in Table 1 and compared with those obtained in Tang *et al.* 2015.

Table 3-c The third dimensionless frequency of the beam with $n = 1$, $r_0 = 0$

		$\lambda 3$			
		$c = 0$	$c = 0.25$	$c = 0.5$	$c = 0.75$
η	1/r	present	present	present	present
0	10	46.4936	43.943	40.4126	35.2629
	30	59.2074	53.1494	46.3266	38.3354
	50	60.765	54.1686	46.9206	38.617
	100	61.4602	54.6166	47.1781	38.7376
	EB	61.6973	54.7684	47.2649	38.7781
5	10	48.947	46.6548	43.4436	38.6914
	30	62.5392	56.5937	49.9090	42.1204
	50	64.207	57.694	50.5578	42.4344
	100	64.9513	58.1776	50.8391	42.5689
	EB	65.2051	58.3414	50.9338	42.614
10	10	55.4945	53.8431	51.3959	47.4791
	30	71.4977	65.7662	59.3121	51.8027
	50	73.4696	67.0859	60.1046	52.1979
	100	74.3493	67.6656	60.448	52.3672
	EB	74.6493	67.862	60.5637	52.424

The results of Table 1 show that rotatory inertia decreases the dimensionless frequencies of the non-rotating Rayleigh beam in comparison to non-rotating Bernoulli-Euler beam. Also, the rotatory inertia is more effective on the dimensionless frequencies of the higher modes of the vibration.

5.2 Beams with linearly varying depth and constant width

The first three dimensionless frequencies of the beam are calculated for four different rotational speed, η =1,2,3,4. It is assumed that $n = 1$, $c = 0.5$, and $r_0 = 0,2$. Setting $n = 1$ in relations (3) corresponds to the beams with linearly varying depth and constant width. For Bernoulli-Euler beam r=0 and for Rayleigh beam $r = \frac{1}{30}$ are applied. The results are tabulated in Table 2 and compared with those obtained by (Tang *et al.* 2015).

The presented results in the Tables 2 present excellent agreement with results obtained by (Tang *et al.* 2015). The results of presented approach in this paper have been obtained with R=8. R is the order of power series (49) which approximate the mode shape function. In Ref (Tang *et al.* 2015), the bending moment function has been approximated by a power series and the results have been obtained with R=10. Therefore, the presented approach in this paper has a more rapid convergence rate in comparison to Ref (Tang *et al.* 2015).

Results of Table 2 show that with increase in the rotational speed η, the dimensionless frequencies of both

Table 4-a The first dimensionless frequency of the beam with $n = 2$, $r_0 = 0$

		λ_1							
		$c = 0$		$c = 0.25$		$c = 0.5$		$c = 0.75$	
η	1/r	present	(Tang *et al.* 2015)	present	(Tang *et al.* 2015)	present	(Tang *et al.* 2015)	present	(Tang *et al.* 2015)
	10	3.4368	3.4368	3.8824	3.8824	4.5517	4.5517	5.7394	5.7394
	30	3.5070	3.5070	3.9483	3.9483	4.6168	4.6168	5.8136	5.8136
0	50	3.5128	3.5128	3.9537	3.9537	4.6221	4.6221	5.8196	5.8196
	100	3.5152	3.5152	3.9559	3.9559	4.6244	4.6244	5.8222	5.8222
	EB	3.51602	3.5160	3.9567	3.9567	4.6252	4.6252	5.8231	5.8231
	10	6.2318	6.2318	6.5881	6.5881	7.1268	7.1268	8.0992	8.0992
	30	6.4251	6.4251	6.7521	6.7521	7.2717	7.2717	8.2436	8.2436
5	50	6.4407	6.4407	6.7654	6.7654	7.2835	7.2835	8.2554	8.2554
	100	6.4473	6.4473	6.7711	6.7711	7.2885	7.2885	8.2604	8.2604
	EB	6.4495	6.4495	6.7729	6.7729	7.2901	7.2901	8.2620	8.2620
	10	10.8187	10.8187	11.1593	11.1593	11.6467	11.6467	12.4866	12.4866
	30	11.1598	11.1598	11.4490	11.4490	11.9083	11.9083	12.7568	12.7568
10	50	11.1870	11.1870	11.4724	11.4724	11.9295	11.9295	12.7788	12.7788
	100	11.1985	11.1985	11.4823	11.4823	11.9385	11.9385	12.7881	12.7881
	EB	11.2023	11.2023	11.4856	11.4856	11.9415	11.9415	12.7912	12.7912

Table 4-b The second dimensionless frequency of the beam with $n = 2$, $r_0 = 0$

		λ_2							
		$c = 0$		$c = 0.25$		$c = 0.5$		$c = 0.75$	
η	1/r	present	(Tang *et al.* 2015)	present	(Tang *et al.* 2015)	present	(Tang *et al.* 2015)	present	(Tang *et al.* 2015)
	10	19.1364	19.1364	18.7656	18.7656	18.2107	18.2107	17.664	17.6638
	30	21.6477	21.6477	20.5475	20.5475	19.3846	19.3846	18.3837	18.3834
0	50	21.8929	21.8929	20.7125	20.7125	19.4885	19.4885	18.4451	18.4449
	100	21.9989	21.9989	20.7832	20.7832	19.5328	19.5328	18.4712	18.4710
	EB	22.0345	22.0345	20.8069	20.8069	19.5476	19.5476	18.4799	18.4797
	10	21.8856	21.8856	21.5647	21.5647	21.0033	21.0033	20.3879	20.3879
	30	24.9737	24.9737	23.7497	23.7497	22.4375	22.4375	21.2664	21.2663
5	50	25.2734	25.2734	23.9509	23.9509	22.5640	22.5640	21.3413	21.3411
	100	25.4026	25.4026	24.0371	24.0371	22.6179	22.6179	21.3731	21.3729
	EB	25.4461	25.4461	24.0660	24.0660	22.6360	22.6360	21.3837	21.3836
	10	28.4787	28.4787	28.3154	28.3154	27.7327	27.7327	26.8986	26.8986
	30	32.9654	32.9654	31.4425	31.4425	29.7521	29.7521	28.1365	28.1364
10	50	33.3940	33.3940	31.7269	31.7269	29.9292	29.9292	28.2418	28.2417
	100	33.5784	33.5784	31.8487	31.8487	30.0046	30.0046	28.2865	28.2864
	EB	33.6404	33.6404	31.8895	31.8895	30.0299	30.0299	28.3014	28.3014

Bernoulli-Euler and Rayleigh beams increase. Also, this change is more intensive for $r_0 = 2$ in compare to $r_0 = 0$. For larger rotational speeds, the variations of the frequencies are more intensive with variations of the r_0.

For the three different rotational speeds, $\eta = 0,5,10$ and four different taper ratios, $c = 0$, 0.25, 0.5, 0.75, the first three dimensionless frequencies of the beam are calculated. It is assumed that hub radius was set to zero ($r_0 = 0$). The results are presented in Tables 3-a to 3-c.

The presented results in the Tables 3 present excellent agreement with results obtained by (Tang *et al.* 2015).

5.3. Beams with linearly varying depth and width

In this example, a rotating beam with linearly varying depth and width, which corresponds to n =2, is assumed. The same dimensionless parameters, as those used in Table 3, are considered and the first three dimensionless frequencies of the rotating beam are calculated. The results are tabulated in Table 4.

The results of Tables 3 and 4 show that with the increase in taper ratio c, the first dimensionless frequency increases and the second and third frequencies decrease. Variations in the dimensionless frequencies are more significant for larger taper ratios.

Table 4-c The third dimensionless frequency of the beam with n = 2, r_0=0

		λ_3							
		c = 0		c = 0.25		c = 0.5		c = 0.75	
η	1/r	present	(Tang *et al.* 2015)	present	(Tang *et al.* 2015)	present	(Tang *et al.* 2015)	present	(Tang *et al.* 2015)
0	10	46.4936	46.4936	44.3682	44.3682	41.4573	41.4572	37.4058	37.4027
	30	59.2074	59.2073	53.6911	53.6911	47.6022	47.6021	40.8291	40.8245
	50	60.7649	60.7649	54.7231	54.7231	48.2205	48.2204	41.148	41.1401
	100	61.4602	61.4601	55.1767	55.1767	48.4887	48.4885	41.280	41.2755
	EB	61.6973	61.6972	55.3304	55.3304	48.5791	48.5789	41.3257	41.3209
5	10	48.9470	48.9470	46.8699	46.8699	44.0143	44.0143	40.0132	40.0105
	30	62.5393	62.5392	56.8774	56.8774	50.6398	50.6397	43.7332	43.7292
	50	64.2069	64.2069	57.9848	57.9848	51.3058	51.3057	44.076	44.0719
	100	64.9513	64.9512	58.4715	58.4715	51.5946	51.5945	44.223	44.2188
	EB	65.2051	65.2050	58.6364	58.6364	51.6919	51.6918	44.2724	44.2681
10	10	55.4945	55.4945	53.5748	53.5748	50.8800	50.8800	46.9575	46.9565
	30	71.4977	71.4977	65.4472	65.4472	58.7877	58.7878	51.4514	51.4492
	50	73.4696	73.4696	66.7598	66.7598	59.5804	59.5805	51.8649	51.8625
	100	74.3493	74.3493	67.3363	67.3363	59.9241	59.9241	52.0422	52.0397
	EB	74.6493	74.6493	67.5316	67.5316	60.0398	60.0399	52.1016	52.0992

Table 5 The first three dimensionless frequency of the beam with n = 1,2, c = 0.5, r_0=0, r=$\frac{1}{100}$

		n=1		n=2	
η		present	(Banerjee and Jackson 2013)	present	(Banerjee and Jackson 2013)
1	λ_1	3.98604	3.9860	4.76325	4.7632
	λ_2	18.4603	18.460	19.6654	19.665
	λ_3	47.3303	47.330	48.6168	48.617
2	λ_1	4.4361	4.4361	5.15546	5.1555
	λ_2	18.9225	18.922	20.058	20.058
	λ_3	47.7836	47.784	48.999	48.999
3	λ_1	5.09176	5.0918	5.7446	5.7446
	λ_2	19.669	19.669	20.696	20.696
	λ_3	48.5293	48.529	49.6298	49.630
4	λ_1	5.8776	5.8776	6.47121	6.4712
	λ_2	20.6693	20.669	21.5579	21.558
	λ_3	49.5537	49.554	50.4991	50.499

5.4 Beams with linearly varying depth and width

For four different rotational speed, η=1,2,3,4, the first three dimensionless frequencies of the beams are calculated. It is assumed that n = 1,2, c = 0.5, r_0 =0, and r=$\frac{1}{100}$. The results are presented in Table 5 and compared with those obtained by (Banerjee and Jackson 2013).

The results of Table 5 present with increase in n parameter the frequencies increase and this change is more significant for lower modes and also, with increase in η parameter, this change decrease. With increase in η parameter the frequencies increase and this change is more significant for n=1 in compare to n=2.

Fig. 3 presents the first five dimensionless frequency curves as a function of the taper ratio c for a rotating Rayleigh beam with n=1, $r = \frac{1}{30}$, r_0=2, η = 5.

Results presented in Fig 3 show their complete consistency with those in Ref. (Tang *et al.* 2015). The results of Fig. 3 present with variations of taper ratio c, the higher modes have more significant non-linear decrease.

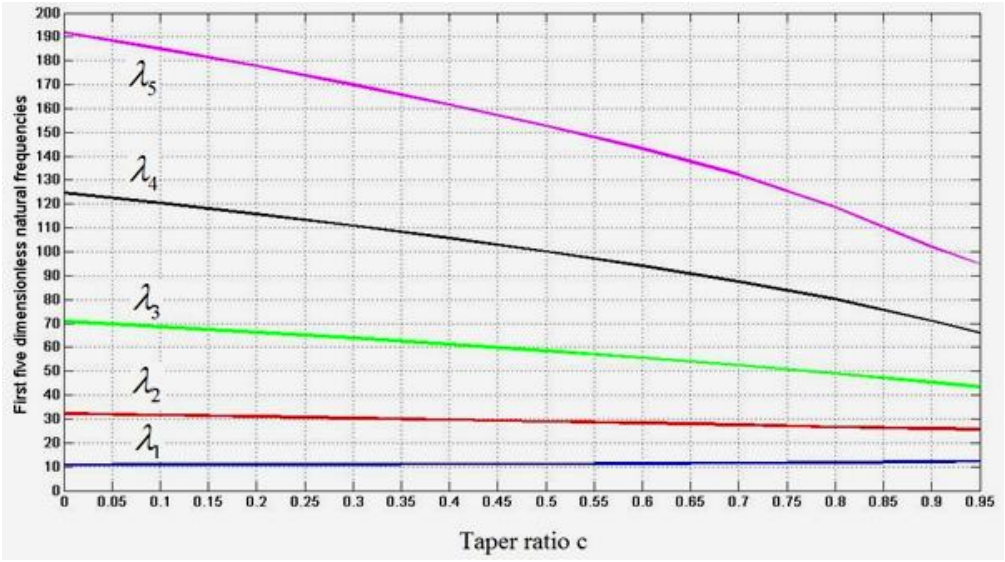

Fig. 3 The first five dimensionless frequency curves as a function of the taper ratio c for a rotating Rayleigh beam with n=1, $r = \frac{1}{30}$, r_0=2, η = 5

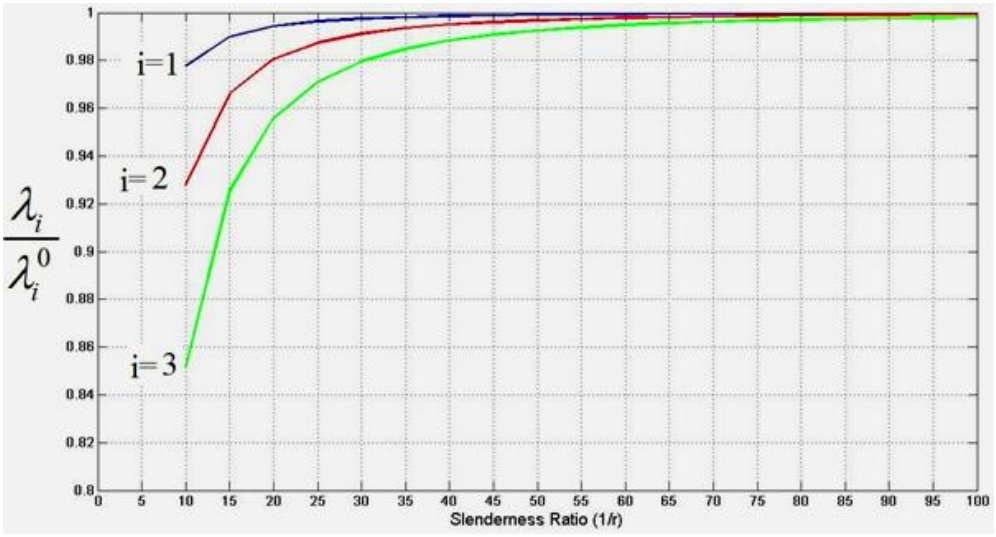

Fig. 4 The first three dimensionless frequency curves of a Rayleigh beam as a function of the slenderness ratio $\frac{1}{r}$ with n=2, c=0.5, r_0=0, η = 5

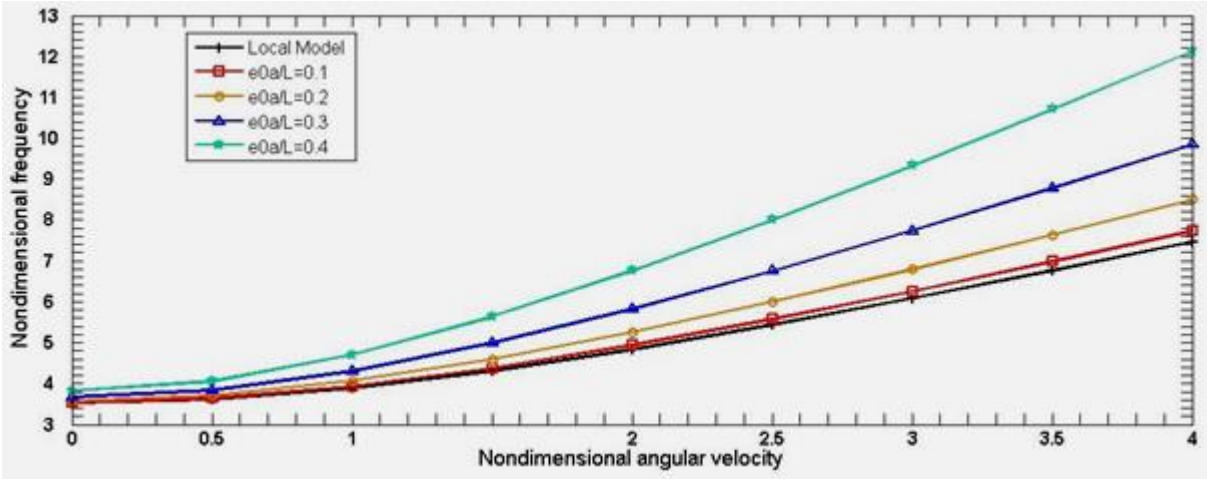

Fig. 5 the variation of the first dimensionless frequency of the beam with dimensionless angular velocity η with r_0=1

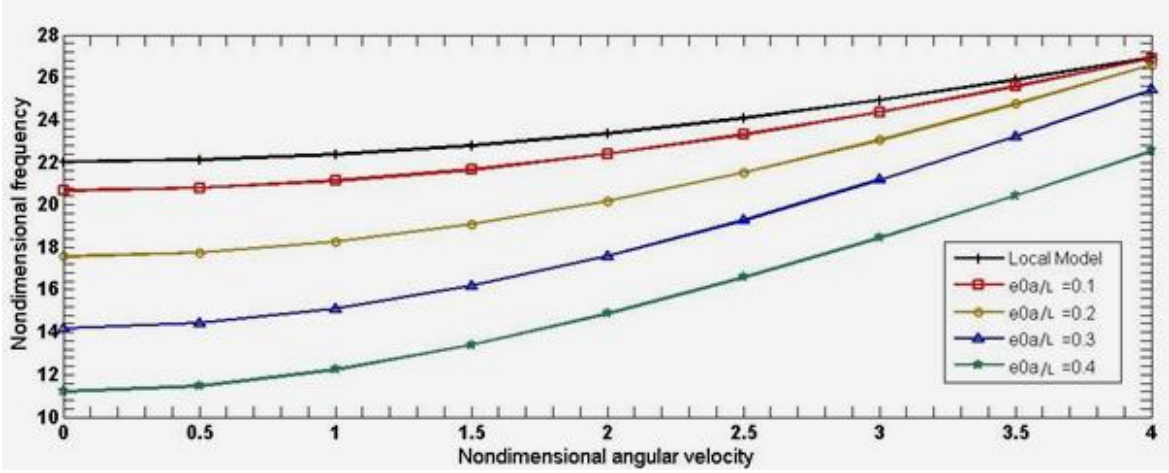

Fig 6 the variation of the second dimensionless frequency of the beam with dimensionless angular velocity η with r_0=1

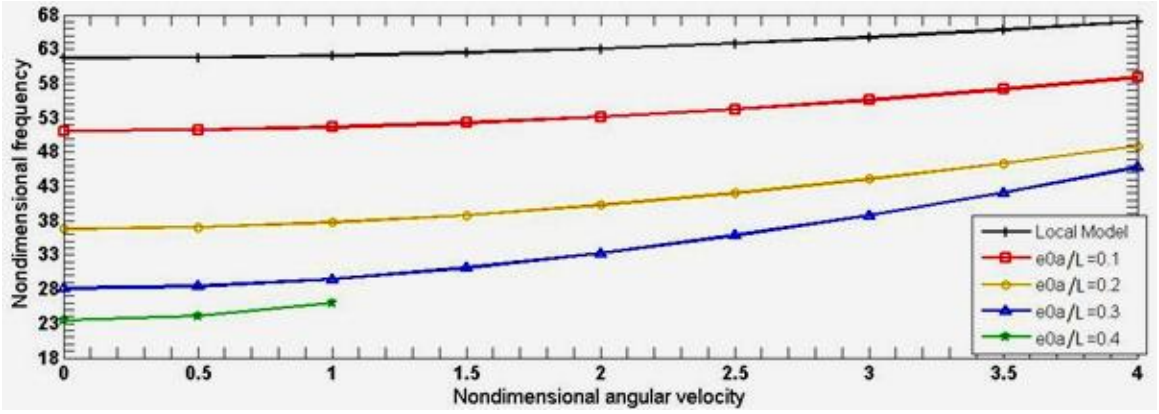

Fig. 7 the variation of the third dimensionless frequency of the beam with dimensionless angular velocity η with r_0=1 and ψ = 0.1, 0.2, 0.3, 0.4

For taper ratio quantities more than 0.75 the decrease in frequencies is intensified. For a rotational speed η=*5*, taper ratio c=0.5, hub-radius r_0 =0, n=2, Fig. 4 shows the ratio between the results obtained by using Rayleigh beam theory (λ_i) and Bernoulli–Euler theory (λ_i^0) for the first three natural frequencies against the slenderness ratio ($\frac{1}{r}$).

Results presented in Fig 4 shows excellent agreement with those in Ref. (Banerjee and Jackson 2013). The results of Fig. 4 present for slenderness ratio less than 25, the variations of the all three modes are more significant. This change is more intensive for higher modes.

5.5 Size-dependency effects

In this example, the effect of size-dependency on the dimensionless frequencies of rotating Euler-Bernoulli beam is investigated. Fig. 5 shows the variation in the first dimensionless frequency of the beam with dimensionless angular velocity η for both local and nonlocal elastic models. For local model, the nonlocal parameter, (ψ=$\frac{e_0 a}{L}$) is assumed to be zero. While for nonlocal model, the nonlocal parameter ψ is assumed to be 0.1, 0.2, 0.3 and 0.4. Here, the dimensionless hub radius is assumed as r_0=1.

The results of Fig. 5 present with increase in η parameter, the frequencies increase and this increase is more intensive for larger ψ. This result says the angular velocity is more effective on the non-local beams and size-dependency effects will be effective with larger angular velocities.

Figs. 6 and 7 show the variation in dimensionless frequency with dimensionless angular velocity for the second and third modes of vibration, respectively. No real Eigen-value has been calculated for the third mode of vibration with ψ = 0.4 beyond η=*1*.

Results of Figs 6 and 7 show that similar to the first mode, with the increase in the angular velocity, the dimensionless frequencies of second and third modes of the vibration increase. But, the results for ψ parameter is different. In compare to the first mode, with increase in the ψ parameter, the second and third frequencies decrease. Fig. 8 shows the variations in the first dimensionless frequency with variations in the dimensionless angular velocity η for different values of dimensionless hub radius, r_0. Four values of hub radius are assumed as: r_0 = 0.5, 1, 1.5, 2. Here, the nonlocal parameter is assumed as: ψ= 0.1.

Fig. 8 shows that with the increase in dimensionless hub radius r_0, the first dimensionless frequency increases. Results presented in Figs 5 to 8 show their complete consistency with those in Ref. (Pradhan and Murmu 2010).

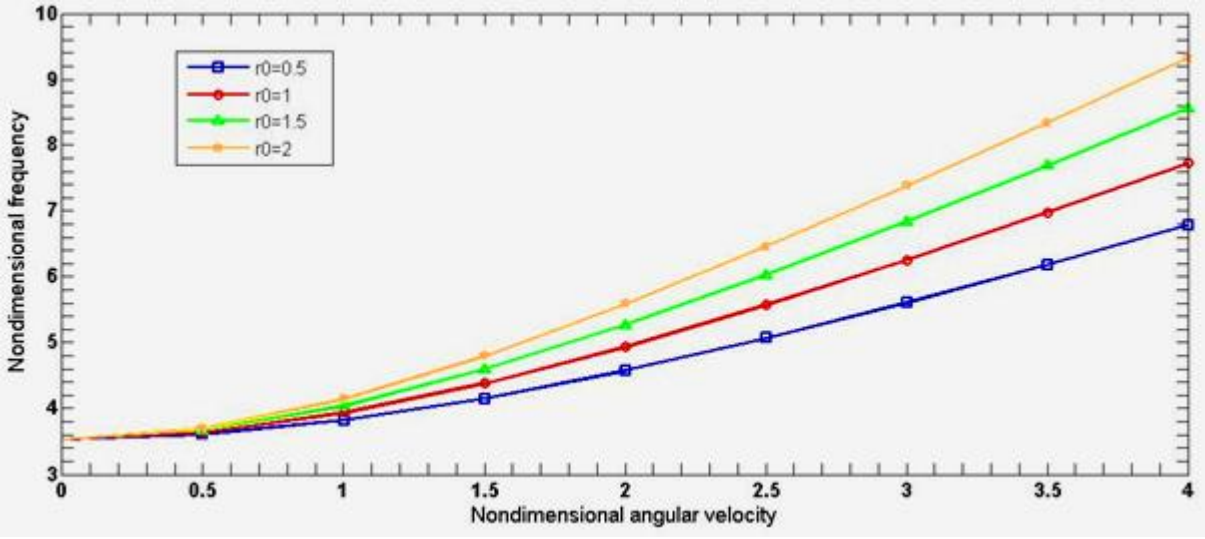

Fig. 8 the variation of the first dimensionless frequency of the beam with dimensionless angular velocity η with $\psi = 0.1$and $r_0 = 0.5, 1, 1.5, 2$

6. Conclusion

Application of the weak form integral equations for flapwise bending vibration of the rotating beams has been presented. Through repetitive integrations, the governing differential equations for flapwise bending vibration of the Rayleigh beam with non-uniform cross section and non-local Euler-Bernoulli beam have been converted into weak form integral equations. In order to solve the resulting integral equations, the mode shape function of the vibration has been approximated by a power series and substitution of the power series into weak form integral equations transformed them into a system of linear algebraic equations. The natural frequencies of the beam have been calculated by determination of a non-trivial solution for system of linear algebraic equations. The accuracy, simplicity and reliability of the proposed method has been verified thorough several numerical examples in which the influence of the geometry properties, rotatory inertia, rotational speed, taper ratio and size-dependency has been investigated on the natural frequencies of the rotating beams. Differences between natural frequencies of proposed method and previous published works were in acceptable ranges. Ref. (Tang *et al.* 2015) was the main reference for comparison of the results obtained. In this reference, the bending moment function has been approximated by a power series with R=10. In the presented approach in this paper, the mode shape function has been approximated by a power series with R=8 which shows more rapid convergence rate.

References

Adhikari, S., Murmu, T. and McCarthy, M.A. (2013), "Dynamic finite element analysis of axially vibrating nonlocal rods", *Finite Element Anal. Design*, **63**, 42–50, http://dx.doi.org/10.1016/j.finel.2012.08.001.

Aranda-Ruiz, J., Loya, J. and Fernández-Sáez, J. (2012), "Bending vibrations of rotating nonuniform nanocantilevers using the Eringen nonlocal elasticity theory", *J. Compos. Struct.*, **94**, 2990–3001, https://doi.org/10.1016/j.compstruct.2012.03.033

Aksencer, T., Aydogdu, M. (2011), "Levy type solution method for vibration and buckling of nanoplates using nonlocal elasticity theory", *Physica E Low-dimensional Syst. Nanostruct.,* **43**, 954–959, https://doi.org/10.1016/j.physe.2010.11.024

Aydogdu, M. (2009), "Axial vibration of the nanorods with the nonlocal continuum rod model", *Physica E Low-dimensional Syst. Nanostruct.,* **41**, 861–864, https://doi.org/10.1016/j.physe.2009.01.007

Banerjee, J.R. and Jackson, D.R. (2013), "Free vibration of a rotating tapered Rayleigh beam: A dynamic stiffness method of solution", *J. Comput. Struct.,* **124**, 11–20, https://doi.org/10.1016/j.compstruc.2012.11.010

Behera, L. and Chakraverty, S. (2015), "Application of Differential Quadrature method in free vibration analysis of nanobeams based on various nonlocal theories", *Comput. Math. Appl.*, **69**, 1444–1462, https://doi.org/10.1016/j.camwa.2015.04.010

Chang, T.P. (2013), "Axial vibration of non-uniform and non-homogeneous nanorods based on nonlocal elasticity theory", *Appl. Math. Comput.*, **219**, 4933–4941. https://doi.org/10.1016/j.amc.2012.11.059

Dehrouyeh-Semnani, A.M. (2015), "The influence of size effect on flapwise vibration of rotating microbeams", *International J. Eng. Sci.,* 94, 150–163, https://doi.org/10.1016/j.ijengsci.2015.05.009

Eltaher, M.A., Emam, S.A. and Mahmoud, F.F. (2012), "Free vibration analysis of functionally graded size-dependent nanobeams", *Appl. Math. Comput.*, **218**, 7406–7420, https://doi.org/10.1016/j.amc.2011.12.090.

Eltaher, M.A., Alshorbagy, A.E. and Mahmoud, F.F. (2013), "Vibration analysis of Euler–Bernoulli nanobeams by using finite element method", *Appl. Math. Model.*, **37**, 4787–4797, https://doi.org/10.1016/j.apm.2012.10.016

Eltaher, M.A., Khairy, A., Sadoun, A.M. and Omar, F.A. (2014), "Static and buckling analysis of functionally graded Timoshenko nanobeams", *Appl. Math. Comput.*, **229**, 283–295, https://doi.org/10.1016/j.amc.2013.12.072

Emam, S.A. (2013), "A general nonlocal nonlinear model for buckling of nanobeams", *Appl. Math. Model.*, **37**, 6929–6939, https://doi.org/10.1016/j.apm.2013.01.043

Eltaher, M.A., Emam, S.A. and Mahmoud, F.F. (2013), "Static and stability analysis of nonlocal functionally graded nanobeams",

Compos. Struct., **96**, 82–88, https://doi.org/10.1016/j.compstruct.2012.09.030

Eltaher, M.A., Khater, M.E., Emam, Samir A. (2016), "A review on nonlocal elastic models for bending, buckling, vibrations, and wave propagation of nanoscale beams", *Appl. Math. Model.*, **40**(5–6), 4109-4128, https://doi.org/10.1016/j.apm.2015.11.026

Eltaher, M.A., Alshorbagy, A.E. and Mahmoud, F.F. (2013), "Determination of neutral axis position and its effect on natural frequencies of functionally graded macro/nanobeams", *Compos. Struct.*, **99**, 193-201, https://doi.org/10.1016/j.compstruct.2012.11.039

Eltaher, M.A., Abdraboh, A.M. and Almitani, K.H. (2018), "Resonance frequencies of size dependent perforated nonlocal nanobeam", *Microsyst. Technol.*, **24**(9), 3925-3937, https://doi.org/10.1007/s00542-018-3910-6

Eltaher, M.A., Abdelrahman, A.A., Al-Nabawy, A., Khater, M., and Mansour, A. (2014), "Vibration of nonlinear graduation of nano-Timoshenko beam considering the neutral axis position", *Appl. Math. Comput.*, **235**, 512-529, https://doi.org/10.1016/j.amc.2014.03.028

Eltaher, M.A., Hamed, M.A., Sadoun, A.M., and Mansour, A. (2014), "Mechanical analysis of higher order gradient nanobeams", *Appl. Math. Comput.*, **229**, 260-272, https://doi.org/10.1016/j.amc.2013.12.076

Ganesh, R. and Ganguli, R. (2013), "Stiff string approximations in Rayleigh–Ritz method for rotating beams", *Appl. Math. Comput.*, **219**, 9282–9295, https://doi.org/10.1016/j.amc.2013.03.017

Ghannadpour, S.A.M., Mohammadi, B. and Fazilati, J. (2013), "Bending, buckling and vibration problems of nonlocal Euler beams using Ritz method", *Compos. Struct.*, **96**, 584–589, https://doi.org/10.1016/j.compstruct.2012.08.024

Huang, C. L., Lin, W. Y. and Hsiao, K. M. (2010), "Free vibration analysis of rotating Euler beams at high angular velocity", *J. Comput. Struct.*, **88**, 991–1001, https://doi.org/10.1016/j.compstruc.2010.06.001

Huang, Y.; Li, X.-F. (2010), "A new approach for free vibration of axially functionally graded beams with non-uniform cross-section", *J. Sound Vib.* **329**(11), 2291–2303, https://doi.org/10.1016/j.jsv.2009.12.029

Kim, H., Yoo, H.H. and Chung, J. (2013), "Dynamic model for free vibration and response analysis of rotating beams", *J. Sound Vib.,* **332**, 5917–5928, https://doi.org/10.1016/j.jsv.2013.06.004

Li, L., Zhang, D.G. and Zhu, W.D. (2014), "free vibration analysis of a rotating hub–functionally graded material beam system with the dynamic stiffening effect", *J. Sound Vib.*, **333**, 1526–1541, https://doi.org/10.1016/j.jsv.2013.11.001

Lee, H.L. and Chang, W.J. (2010), "Surface and small-scale effects on vibration analysis of a nonuniform nanocantilever beam", *Physica E Low-dimensional Syst. Nanostruct.,* **43**, 466–469, https://doi.org/10.1016/j.physe.2010.08.030

Murmu, Y. L., Adhikari, S. and Friswell, M.I. (2013), "Dynamic characteristics of damped viscoelastic nonlocal EulereBernoulli beams", *Europe. J. Mech. A/Solids*, **42**, 125-136, https://doi.org/10.1016/j.euromechsol.2013.04.006

Murmu, T. and Pradhan, S.C. (2009), "Small-scale effect on the vibration of nonuniform nanocantilever based on nonlocal elasticity theory", *Physica E Low-dimensional Syst. Nanostruct.*, **41**, 1451–1456, https://doi.org/10.1016/j.physe.2009.04.015

Mohammadnejad, M. (2015), "A new analytical approach for determination of flexural, axial and torsional natural frequencies of beams", *Struct. Eng. Mech.*, **55**(3), 655-674, https://doi.org/10.12989/sem.2015.55.3.655

Nguyen, N.T., Kim, N.I., Lee, J. (2015), "Mixed finite element analysis of nonlocal Euler–Bernoulli nanobeams", *Finite Element Anal. Design*, **106**, 65–72, https://doi.org/10.1016/j.finel.2015.07.012

Narendar, S. (2012), "Differential quadrature based nonlocal flapwise bending vibration analysis of rotating nanotube with consideration of transverse shear deformation and rotary inertia", *Appl. Math. Comput.*, **219**, 1232–1243, https://doi.org/10.1016/j.amc.2012.07.032

Niknam, H. and Aghdam, M.M., "A semi analytical approach for large amplitude free vibration and buckling of nonlocal FG beams resting on elastic foundation" *Compos. Struct.*, http://dx.doi.org/10.1016/j.compstruct.2014.09.023.

Phadikar, J.K. and Pradhan, S.C. (2010), "Variational formulation and finite element analysis for nonlocal elastic nanobeams and nanoplates", *Comput. Mater. Sci.*, **49**, 492–499, https://doi.org/10.1016/j.commatsci.2010.05.040

Pradhan, S.C. and Murmu, T. (2010), "Application of nonlocal elasticity and DQM in the flapwise bending vibration of a rotating nanocantilever", *Physica E: Low-dimensional Systems and Nanostructures*, **42**, 1944–1949, https://doi.org/10.1016/j.physe.2010.03.004

Salehipour, H., Nahvi, H. and Shahidi, A. R. (2014), "Exact analytical solution for free vibration of functionally graded micro/nano plates via three-dimensional nonlocal elasticity", *Physica E Low-dimensional Syst. Nanostruct.*, http://dx.doi.org/10.1016/j.physe.2014.10.001.

Saffari, H., Mohammadnejad, M., and Bagheripour,MH. (2012), "Free vibration analysis of non prismatic beams under variable axial forces", *Struct. Eng. Mech.,* **43**(5), 561-582, http://dx.doi.org/10.12989/sem.2012.43.5.561

Saffari, H. and Mohammadnejad, M. (2015), "On the application of weak form integral equations to free vibration analysis of tall structures", *Asian J. Civil Eng. (BHRC),* **16**(7), 977-999.

Salehipour, H., Shahidi, A.R. and Nahvi, H. (2015), "Modified nonlocal elasticity theory for functionally graded materials", *International J. Eng. Sci.*, **90**, 44–57, https://doi.org/10.1016/j.ijengsci.2015.01.005

Thai, H.T. (2012), "A nonlocal beam theory for bending, buckling, and vibration of nanobeams", *J. Eng. Sci.*, **52**, 56–64, https://doi.org/10.1016/j.ijengsci.2011.11.011

Thai, H.T., Vo, T.P. (2012), "A nonlocal sinusoidal shear deformation beam theory with application to bending, buckling, and vibration of nanobeams", *J. Eng. Sci.*, **54**, 58–66, https://doi.org/10.1016/j.ijengsci.2012.01.009

Tang, A.-Y., Li, X.-F., Wu, J.-X. and Lee, K.Y. (2015), "Flapwise bending vibration of rotating tapered Rayleigh cantilever beams", *J. Construct. Steel Res.,* **112**, 1-9, https://doi.org/10.1016/j.jcsr.2015.04.010

CC